Dalton Transactions

ROYAL SOCIETY OF CHEMISTRY

PAPER

View Article Online
View Journal | View Issue

Cite this: *Dalton Trans.*, 2024, **53**, 17554

A UV-Vis method for investigation of gallium(III) complexation kinetics with NOTA and TRAP chelators: advantages, limitations and comparison with radiolabelling†

Viktor Lebruška, [a] Tereza Dobrovolná, [a] Tereza Gemperle,[a] Vojtěch Kubíček, *[a] Susanne Kossatz[b] and Petr Hermann [a]

An easy and cheap method for measurement of Ga^{III} complexation kinetics was developed. The method is based on UV-Vis quantification of non-complexed chelators after the addition of Cu^{II} ions at individual time points. The method was evaluated using established ligands, H_3nota and H_6notP^{Pr}, and was utilized to study the kinetics of Ga^{III} complexation with four new symmetric derivatives of 1,4,7-triazacyclononane bearing methylphosphonate/phosphinate pendant arms – TRAP ligands. Chelators bearing ethoxy groups (H_3**L^1**) or 2,2,2-trifluoroethyl groups (H_3**L^2**) on the phosphorus atoms showed fast formation ($t_{99\%}$ = 21 and 10 min, respectively, at pH 2.0) and efficient radiolabelling which were comparable to the previously reported chelators bearing the 2-carboxyethyl group (H_6notP^{Pr}). Chelators bearing (*N*,*N*-dibenzyl-amino) methyl (H_3**L^3**) and aminomethyl (H_3**L^4**) substituents showed a significantly slower complexation ($t_{99\%}$ = 4.4 and 3.6 h, respectively, at pH 2.0) and inefficient radiolabelling, mainly at room temperature or low pH. This was caused by protonation of the amino groups of the pendant arms leading to coulombic repulsion between the Ga^{III} ion and the positively charged protonated amines. The trends in complexation rates determined by the UV-Vis method correlated well with the results of the ^{68}Ga radiolabelling study.

Received 21st August 2024,
Accepted 1st October 2024

DOI: 10.1039/d4dt02383h

rsc.li/dalton

Introduction

Current medicine uses various imaging techniques based on ionizing radiation. One of them is positron emission tomography (PET), a non-invasive technique used for selective imaging of tissues, typically in combination with magnetic resonance imaging (MRI) or computed tomography (CT). PET utilizes positron-emitting radioisotopes. The emitted positron annihilates with an electron from the surrounding tissue and generates a photon pair. The simultaneous formation and detection of two photons offers high sensitivity and resolution. Detection of the photons allows for the reconstruction of the radioisotope distribution in tissues.

Production of the most common β^+ radioisotopes is based on cyclotrons. This represents a drawback, due to the high costs of purchase and maintenance of the cyclotrons. Thus, portable radioisotope generators attract increasing attention. Among them, commercial ^{68}Ga/^{68}Ge generators provide a source of the positron emitter ^{68}Ga (89% β^+; $\tau_{1/2}$ = 67.7 min; $E_{max}(\beta^+)$ = 1.90 MeV) for PET imaging.[1,2] They are available from several vendors and versatile in their use, making ^{68}Ga one of the most widely used imaging radioisotopes.

The free Ga^{III} aqua-ion exhibits non-specific deposition in tissues and, thus, it must be bound in thermodynamically stable and kinetically inert complexes which are often conjugated to biologically active vectors to ensure their specific accumulation in tissues. There are several important parameters for the chelator to be used as a ^{68}Ga carrier, such as charge, hydrophilicity/hydrophobicity, very fast, selective and quantitative Ga^{III} complexation, and solubility and stability in body fluids. To meet these requirements, the chelator must be finely designed in terms of the number and kind of donor groups, overall complex charge, geometry of the coordination sphere, *etc*.

Commonly used chelators for Ga^{III} complexation are analogues of H_4dota (1,4,7,10-tetraazacyclododecane-1,4,7,10-tetraacetic acid) and H_3nota (1,4,7-triazacyclononane-1,4,7-tri-

[a]*Department of Inorganic Chemistry, Faculty of Science, Charles University in Prague, Hlavova 2030, 128 40 Prague, Czech Republic. E-mail: kubicek@natur.cuni.cz; Tel: +420221951436*
[b]*Department of Nuclear Medicine, TUM University Hospital and Central Institute for Translational Cancer Research (TranslaTUM), School of Medicine, Technical University Munich (TUM), Einsteinstrasse 25, 81675 Munich, Germany*

†Electronic supplementary information (ESI) available: Examples of UV-Vis and NMR kinetic data, NMR and MS spectra of ligands and complexes, overall protonation constants, complexation rate constants and times. See DOI: https://doi.org/10.1039/d4dt02383h

acetic acid). However, H_4dota is not optimal for Ga^{III} complexation as its macrocyclic cavity is too large and the number of donor atoms exceeds the number (six) of Ga^{III} coordination sites.[3] In addition, Ga^{III} complexes with H_4dota and its derivatives often show slow complexation/radiolabelling and limited *in vivo* stability. In contrast, the compact ligand cavity of H_3nota is well pre-organized for the octahedral coordination of small ions and a lot of chelators derived from 1,4,7-triazacyclononane (tacn) have been used for Ga^{III} complexation.[4,5] Promising properties were reported for tacn-based chelators with three methylphosphinate pendant arms, called TRAP chelators.[6] The phosphinic acid pendant arms become deprotonated at a pH lower than the carboxylic pendants and ring nitrogen atoms of phosphinate-bearing macrocycles are less basic than those in acetate-bearing H_3nota. Therefore, phosphonate/phosphinate chelators mostly coordinate Ga^{III} faster and at a lower pH than their acetate analogue.[7–10] Various TRAP chelators bearing different groups attached to the phosphorus atom have been synthesized and studied for complexation of the Ga^{III} ion. The chelators bearing 2-carboxyethyl or hydroxomethyl groups (H_6notP^{Pr}, H_3notP^{hm} and H_4nopo in Fig. 1) showed a fast complexation and a very good radiolabelling efficiency,[6,9,11] whereas Ga^{III} binding by TRAP chelators bearing hydrogen atoms or phenyl groups (H_3notP^{H} and H_3notP^{Ph}) was much less effective.[12] However, factors influencing the Ga^{III} complexation are not fully understood.

As the complexation rate is a key property of chelators used as carriers of radioisotopes, significant attention is usually focused on the measurement of complexation kinetics. The most common method used to follow complexation kinetics is UV-Vis spectroscopy. However, the Ga^{III} ion shows no UV-Vis absorption. The complexation kinetics of such complexes must be studied by a different method. Therefore, previously reported data on the formation of Ga^{III} complexes were mostly obtained by ^{31}P and/or ^{71}Ga NMR spectroscopy.[3,12–14] However, the NMR experiments require high concentrations of the studied compounds and long data acquisitions. The acquisition times are typically at least minutes and, thus, only reaction kinetics running in timespans of tenths of minutes can be investigated by NMR. In addition, kinetic experiments are time-consuming which is often incompatible with the available NMR time. Thus, the published kinetic data are scarce and only a few complexation mechanistic studies have been reported.[12,14,15]

Another option for studying the complexation of ions having no UV-Vis absorption is by using indirect methods using a "visualization agent".[16–19] The experiments were mostly performed by the addition of complexing dyes (chelatometric indicators) into the reaction mixture. However, in such arrangement, the dye must be used in excess and, thus, it binds the metal ion and changes its rate of complexation by the studied ligand. This problem is typically solved by variation of the dye concentration and the linear extrapolation of reaction rates to zero dye concentration. However, the extrapolation introduces significant uncertainty as the linearity might not be maintained at low dye concentrations.

In order to avoid the above-mentioned limitations, we developed a new method for UV-Vis quantification of the reaction progress. It is a batch method based on addition of Cu^{II} ions in excess to the reaction solution at individual time points. The complexation of Cu^{II} ions by the remaining free ligand quenches the Ga^{III} complexation and the quantification of the formed Cu^{II} complex allows us to determine the Ga^{III} complexation extent. The method was first evaluated using established ligands, H_3nota and H_6notP^{Pr} (Fig. 1) and, furthermore, it was utilized to study the kinetics of Ga^{III} complexation with four new symmetric derivatives of tacn bearing methylphosphonate/phosphinate pendant arms – TRAP ligands – to evaluate the effect of the phosphorus atom substituents (Fig. 1). The ligands $H_3\mathbf{L}^1$ bearing ethoxy groups (*i.e.* phosphonate monoester moiety), $H_3\mathbf{L}^2$ 2,2,2-trifluoro-ethyl groups and $H_3\mathbf{L}^3$ *N*,*N*-dibenzyl-aminomethyl groups are chelators with an increased lipophilicity. The effect of the hydrophilic and positively charged amino groups was evaluated comparing $H_3\mathbf{L}^3$ and $H_3\mathbf{L}^4$ bearing aminomethyl groups. To the best of our knowledge, this is the first work systematically studying the kinetics of the Ga^{III} complexation.

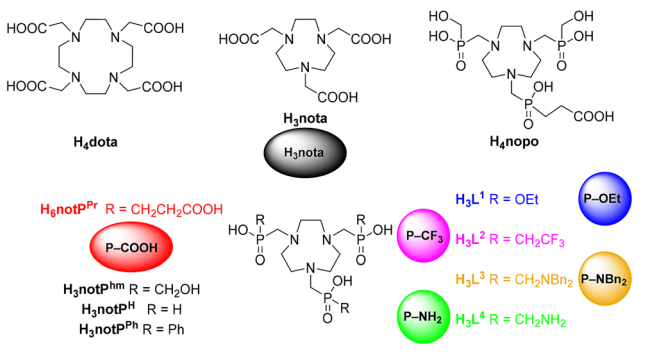

Fig. 1 Discussed chelators (the colors and pictograms serve an easier orientation in the Results section).

Methodology

The UV-Vis method for investigation of Ga^{III} complexation kinetics

In order to gather data necessary for the evaluation of Ga^{III} complexation kinetics, we sought a suitable and cheap method, and UV-Vis spectroscopy is the method of the first choice. However, neither the Ga^{III} ion nor the studied chelators showed any absorption bands in the UV-Vis region. Thus, an indirect method must be used. The previously reported indirect methods used dyes to visualize metal ions.[16–19] The dyes were added directly to the reaction mixture so the metal ion was not present in the solution in a free (*i.e.* aqua-ion) form but as a complex with the dye. The metal ion–dye interaction significantly changed the availability of the metal ion for complexation by the investigated chelator. To overcome this issue, we propose a batch method in which the

"visualization" agent was not added into the reaction mixture but it was added into the analyzed solution just before the UV-Vis measurement and it also quenches the studied complexation reaction. We first tested several dyes (*e.g.* Arsenazo III, xylenol orange) to visualize the "free" metal aqua-ion and none of them was suitable for the batch method due to a long time necessary to reach full equilibrium after addition of the dye. Finally, we developed a method, which did not visualize the free metal ion but the free ligand by the addition of a Cu^{II} ion. The added Cu^{II} was immediately bound by the free ligand resulting in the formation of a complex with significant UV-Vis absorption allowing precise quantification of the reaction extent.

The method was first tested on the parent ligand, H_3nota. The solution containing Ga^{III} and H_3nota was incubated at 30 °C under desired conditions, an aliquot of the solution was taken at each time point and quickly mixed with an excess of Cu^{II} ions. The Cu^{II} ion is known to show very fast complexation by H_3nota.[20,21] This reaction is several orders of magnitude faster than the reaction of H_3nota with the Ga^{III} ion[12] and, thus, any free chelator immediately bound Cu^{II} ions. After the Cu^{II} addition, the complexation processes were immediately stopped and the extent of the reaction was evaluated by quantification of the Cu^{II} complex concentration which equaled the concentration of the free non-complexed chelator. Thus, the progress of the reaction with Ga^{III} could be easily quantified from the intensity of the absorption band of the formed Cu^{II} complex. The ligand-to-metal charge transfer (LMCT) band at ~270 nm was used for the quantification as it showed a significantly higher intensity than a broad d–d transition band in the visible region. An example of the original kinetic data and their treatment is shown in Fig. S1.†

After the addition of Cu^{II} salt, the metal ion was present in an excess over the chelator. Thus, possible transmetallations after the quenching of the reaction had to be excluded. To ensure this, each Cu^{II} and Ga^{III} complex was treated with ten-times excess of the other metal ion and no transmetallation was observed for 30 min under the same conditions as those used for the quenching reactions; this time period provided enough time to perform the UV-Vis measurement of the solution. The Cu^{II} ion did not replace the Ga^{III} ion in the complex due to thermodynamic reasons ($\log K_{[Ga(nota)]} = 29.6$,[12] $\log K_{[Cu(nota)]} = 23.3$[20]), whereas the Ga^{III} ion did not replace the Cu^{II} ion in its complex due to kinetic reasons; Ga^{III} complexation by the free ligand is relatively slow and it is even much slower if the ligand cavity is blocked by the Cu^{II} ion (the transmetallation reaction is extremely slow).

To demonstrate that the method can also be used for TRAP ligands and to independently validate the suggested UV-Vis method, Ga^{III} complexation with $H_3\mathbf{L^2}$ was followed at pH 1 by ^{1}H NMR under identical conditions (Fig. S2†). Ligand $H_3\mathbf{L^2}$ was chosen as the methylene signal of its trifluoroethyl group was not affected by excitation sculpting used to suppress the water signal. The rate constants were almost identical in both experiments (NMR: $k_{obs} = 2.8(2) \times 10^{-4}$ s^{-1}; UV-Vis: $k_{obs} = 2.7(2) \times 10^{-4}$ s^{-1}) and, thus, the direct NMR measurement fully confirmed the accuracy of the UV-Vis method used.

The developed method is not universal and has several limitations:

(i) The most important requirements are a suitable Cu^{II} complexation rate and transmetallation rates in both directions. The Cu^{II} complexation rate must be at least two orders of magnitude faster than that of the metal ion in question so that the progress of complexation with the studied metal ion is negligible during the formation of the Cu^{II} complex. Additionally, transmetallation must be slow enough to avoid any mutual transformation of the species during the sample manipulation and spectral measurements. The knowledge of Cu^{II} complexation and transmetallation kinetics does require additional preliminary experiments. However, detailed quantitative data are not necessary to obtain, and qualitative experiments can be easily and quickly obtained using UV-Vis measurements.

(ii) The ligand should form complexes of sufficient stability with both, Cu^{II} and the metal ion in question. However, the stability of the Cu^{II} complex might be lower than that of the studied metal ion as the decisive factors are the complexation and transmetallation rates.

(iii) Thermodynamic stability of the complexes is important for quantitative formation of complexes, mainly under strongly acidic conditions. This requirement must be met for the studied metal ion but it is not crucial for the Cu^{II} complex. Quenching of the reaction can be done with Cu^{II} excess and in solution buffered at a different pH from that of the kinetic experiments. This was also our approach. To ensure quantitative Cu^{II} complexation, Cu^{II} solution buffered at pH 3 was used for quenching the reaction and the consequent spectral measurements. Our experiments showed that there is no influence of pH of the Cu^{II} solution (tested in the range 2–4) on the data obtained.

(iv) Another factor is the ligand-to-metal stoichiometry. In the optimal case, the stoichiometry of the Cu^{II} complex and the complex of the studied metal ions should be the same. However, this is not an absolute requirement as the relative change in spectra is the measure of the reaction progress and it should not be dependent on the complex stoichiometry.

The method could be used not only for the investigation of the Ga^{III} complexation but also for kinetic investigations of other metal ions having no UV-Vis absorption. The requirements described above indicate that the method shows high potential mainly for the complexation of trivalent metal ions with macrocyclic ligands. Trivalent metal ions form typically complexes much more slowly than Cu^{II} and their complexes with macrocyclic ligands are often kinetically inert and, thus, they undergo only slow dissociation and transmetallation reactions. The prospective members of this group are Sc^{III}, Y^{III}, In^{III}, La^{III} or Lu^{III}, all of them being of high radiochemical interest.

The high intensity of the CT band of the studied Cu^{II} complexes allows us to perform the experiments in millimolar or even sub-millimolar concentrations of the reactants. The method could be used for kinetic measurements performed at

various ligand-to-metal ratios. There is no limit to the metal ion excess used. However, a high ligand excess would decrease the sensitivity of the method as the amount of Ga^{III}-bound ligand is too small with respect to the overall amount of the ligand bound in the Cu^{II} complex formed after quenching. The limit of the method regarding rates of studied processes is given by the time required to transfer a precise volume of the studied solution to the solution containing Cu^{II} ions. This can be managed in a few seconds and allows the method to be used for investigation kinetics with half-times significantly lower than one minute. As mentioned earlier, the advantage of the described batch quenching method is that Cu^{II} ions are not present in the reaction mixture in the course of the investigated complexation process and, therefore, do not alter the complexation reaction and measured complexation rate. A disadvantage of the experiment is that it requires the continuous presence of the researcher through the measurements. However, this disadvantage could be overcome by automation using *e.g.* flow injection analysis.

In this work, we used the method to investigate the rates of complexation reactions of Ga^{III} with H_3nota and several phosphinic acid analogues. The H_3nota derivatives and their complexes were expected to behave analogously to H_3nota, except for the complexation rate. The phosphinic acid derivatives have a similar difference in Ga^{III} and Cu^{II} stability constants as H_3nota (*e.g.* $\log K_{[Ga(notPPr)]} = 26.24$ and $\log K_{[Cu(notPPr)]} = 16.85$)[6] and the Cu^{II}–Ga^{III} mutual transmetallation reactions are very slow. The method allowed the use of relatively low sub-millimolar concentrations of the reactants. As radiochemical labelling is typically performed under a large chelator excess, the measurements described in this work were performed under a ligand excess; however, only a two-fold ligand excess was used to maintain a high sensitivity of the measurements.

Results and discussion

Synthesis of chelators and Ga^{III} complexes

Chelators were synthesized by Mannich-type reactions of the corresponding organophosphorus precursors with tacn (1,4,7-triazacyclononane) and paraformaldehyde (Fig. 2). All chelators were characterized by NMR, MS and EA (Fig. S3–S6†). The ligand $H_3\mathbf{L^1}$ was prepared by a two-step procedure. In the first step, fully esterified intermediate **1** was synthesized by a Mannich-type reaction with an excess of triethyl phosphite (used as a solvent). Ion-exchange workup yielded a crude intermediate **1** (~90% yield) which was subsequently treated with aq. NaOH to selectively hydrolyze one ester group. Purification on a strong cation exchanger followed by lyophilization yielded $H_3\mathbf{L^1}$ as a hygroscopic powder in 47% yield (based on tacn). Ligand $H_3\mathbf{L^1}$ was earlier synthesized by a different approach.[22] In the first step, **1** was prepared by the reaction of tacn with diethyl phosphite and paraformaldehyde in benzene and the second step was similar to our procedure. Our method achieved a slightly higher yield than the reported one (41% based on tacn), while eliminating the use of carcinogenic benzene as a solvent.

The ligand $H_3\mathbf{L^2}$ was synthesized in a single step according to a published procedure.[23] Starting from tacn with a slight excess of (2,2,2-trifluoroethyl)-H-phosphinic acid (**2**) and paraformaldehyde, $H_3\mathbf{L^2}$ was formed with 85% conversion according to ^{31}P NMR. A side-product was the macrocycle bearing two pendant arms. After chromatography on silica and ion exchange workup, the product was obtained in 71% yield.

Synthesis of $H_3\mathbf{L^3}$ and $H_3\mathbf{L^4}$ started from [(*N*,*N*-dibenzyl)-aminomethyl]-H-phosphinic acid (**3**).[24] Using a slight excess of **3** and paraformaldehyde, $H_3\mathbf{L^3}$ was formed quantitatively according to ^{31}P NMR and it was isolated in 84% yield after ion exchange workup and lyophilization. $H_3\mathbf{L^4}$ was synthesized by

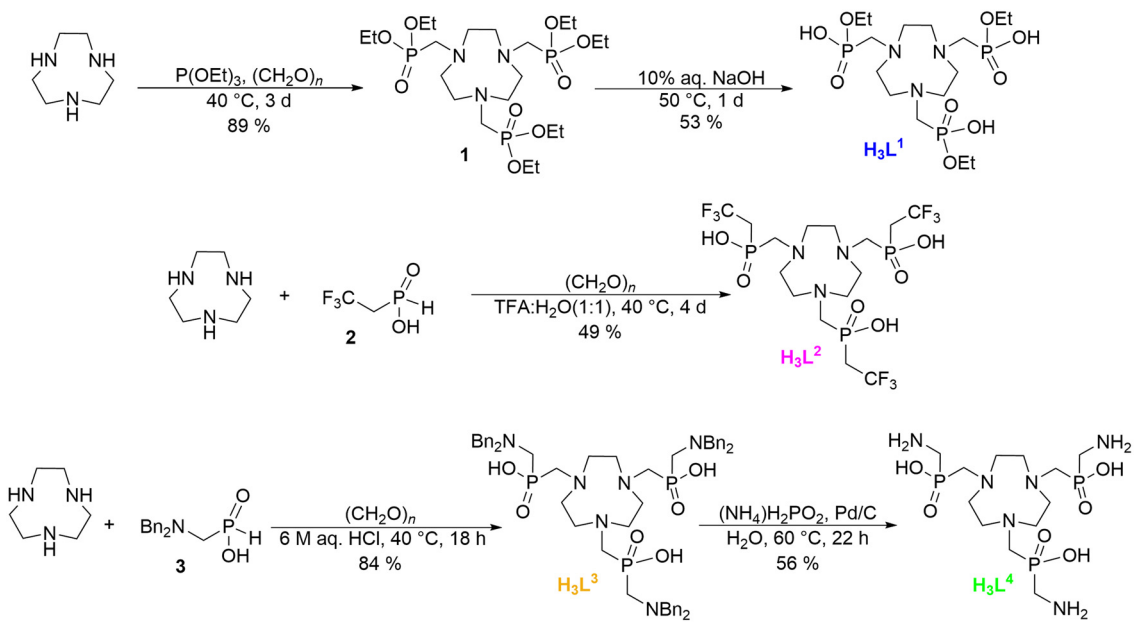

Fig. 2 Synthesis of the studied chelators.

reductive cleavage of the benzyl groups of $H_3\mathbf{L^3}$ on the Pd/C catalyst. The reaction is very sensitive as the utilization of inappropriate conditions (temperature, H_2 gas pressure, pH, solvent, hydrogen source) easily led to N–C–P fragment cleavage and pendant arm degradation. Quantitative debenzylation with minimal degradation was reached in diluted aqueous ammonia using ammonium hypophosphite as a hydrogen source and at room temperature. After catalyst filtration and ion exchange workup, $H_3\mathbf{L^4}$ was isolated by lyophilization in 56% yield (based on $H_3\mathbf{L^3}$). Solutions of **Ga–L^1** and **Ga–L^2** complexes were prepared by stirring a freshly prepared suspension of $Ga(OH)_3$ in the chelator solution overnight. The $Ga(OH)_3$ excess was filtered off through a microfilter, yielding stock solutions of the complexes. The **Ga–L^4** solution was prepared by mixing the chelator solution with an excess of $Ga(NO_3)_3$ at pH 3.5. Then, pH was raised to 5.6 leading to the precipitation of the excessive Ga^{III} in the form of $Ga(OH)_3$ which was filtered off. The solutions of **Ga–L^1**, **Ga–L^2** and **Ga–L^4** complexes were characterized by NMR and HRMS (Fig. S7–S12†). Chelator $H_3\mathbf{L^3}$ formed an insoluble complex with Ga^{III} precipitating from the reaction mixture. The **Ga–L^3** complex was not characterized by spectroscopic techniques due to its very low solubility in common solvents.

^{1}H NMR spectra of the studied Ga^{III} complexes contained a number of split or broad signals (Fig. S7, S9 and S11†). This could be ascribed to the decreased ligand symmetry after the Ga^{III} complexation and/or the presence and interconversion of isomers of the complexes. In complexes of NOTA-like ligands, the pendant arms are twisted clock-wise or anticlock-wise with the respect to the macrocrocycle chelate ring conformation and, thus, the complexes are chiral.[25] As a result, the hydrogen atoms in all ligand methylene groups become nonequivalent. In addition, the coordination of phosphinates or phosphonate monoesters to a metal ion introduces other chirality centers on the phosphorus atoms.[6,12,26–28] Thus, the complexes often form a mixture of diastereoisomers in solution that typically undergo mutual interconversion. The isomeric composition and the interconversion were difficult to study by ^{1}H NMR due to the mentioned signal broadening and splitting. The ^{31}P and ^{19}F NMR (for **Ga–L^2**) spectra provided better information on the speciation of the complexes in solution.

The **Ga–L^1** complex showed two major signals in the ^{31}P NMR spectra at room temperature. These diastereomers could not be distinguished in ^{71}Ga NMR due to the very similar coordination environment formed by the chelator in all species. The presence of two (or more) diastereomers also resulted in very complicated ^{1}H NMR spectra. At an elevated temperature (90 °C, Fig. S7b†), the spectra became simpler confirming the mutual interconversion of the diastereomers. However, the broad signals showed that the interconversion proceeded on the NMR time scale even at an elevated temperature. In contrast, only one dominant signal was found in ^{31}P NMR spectra of the **Ga–L^2** and **Ga–L^4** complexes. The different diastereomeric composition of complexes of each chelator could result from a mutual interaction of the pendant arms (*e.g.* with assistance of hydrogen bonds) or from the preferential formation of some diastereomers in the course of complexation which might be related to the geometry of complexation intermediates. The obtained results agreed with the previously reported formation of the diastereomeric mixture in the complexes of H_3nota and H_4dota analogues with the phosphonate monoester pendant arms, whereas complexes of ligands with the phosphinate pendants preferentially formed one diastereomer.[12,27–29]

Protonation constants of ligands

A key step of metal ion complexation by NOTA-like ligands is deprotonation of the macrocycle amino groups. Thus, the protonation constants of $H_3\mathbf{L^1}$ and $H_3\mathbf{L^4}$ were determined by potentiometry. The results are compiled and compared with data from the literature for other ligands in Tables 1 and S1.† The protonation constants of $H_3\mathbf{L^3}$ were not determined due to the limited ligand solubility in the neutral pH region.

In all ligands, the first protonation was localized on the macrocycle amine groups and occurred in the alkaline region (10–13). The first protonation constant of H_3nota was significantly higher than that of all phosphinate ligands. It agreed with the common trend in ligand basicity where amino groups in amino-phosphinates are less basic than those in amino-carboxylates.[30] $H_3\mathbf{L^2}$ showed the lowest basicity due to the electron-withdrawing effect of the fluorine atoms extending to the ring nitrogen atoms. The further protonation(s) of the ligands occurred in the acidic region. In $H_3\mathbf{L^1}$, $H_3\mathbf{L^2}$ and the simple analogues H_3notP^{hm} and H_3notP^{H}, it corresponded to the second macrocycle amine protonation. In H_3nota and H_6notP^{Pr} showing several protonation constants in the acidic

Table 1 Stepwise ($\log K_a$) protonation constants of the studied and similar ligands and stability constants of their complexes (I = 0.1 M $(NMe_4)Cl$, 25 °C)

Species	H_3nota[12,20]	H_6notP^{Pr} [6]	$H_3\mathbf{L^1}$ [a]	$H_3\mathbf{L^2}$ [23]	$H_3\mathbf{L^4}$	H_3notP^{hm} [12]	H_3notP^{H} [12]
HL	13.17	11.48	11.54	10.23	11.21	11.47	10.48
H_2L	5.74	5.44	3.43	2.86	8.84	3.85	3.28
H_3L	3.22	4.84	1.40	—	8.16	1.30	~1.1
H_4L	1.96	4.23	—	—	7.30		
H_5L	0.70	3.45	—	—	2.09		
H_6L	—	1.66	—	—	—		
$\sum\log K_N$	18.91	14.93	14.97	13.09	13.30	15.32	13.76
$\log K_{[Ga(L)]}$	29.63	26.24	20.5	—	—	23.3	21.91
$\log K_{[Cu(L)]}$	23.33	16.85	14.7	—	—	15.53	13.43

[a] For a full set of stability constants see Table S2.†

region, it corresponded to the protonation of the carboxylate groups and to the second protonation of the macrocycle amines. The phosphinate-bound methylamino groups of $H_3\mathbf{L^4}$ were protonated in the weakly alkaline region (pH 7–9) and the close values of all three aminomethyl protonation constants indicated that the protonations are more or less independent. The phosphinic acid groups were highly acidic and phosphinates were protonated only in strongly acidic solutions. Thus, not more than one protonation constant corresponding to the protonation of the phosphinate groups of each ligand could be determined by potentiometry.

Ga^{III} complexation kinetic data

The UV-Vis method described above was used to investigate Ga^{III} complexation kinetics with H_3nota, H_6notP^{Pr} and the title chelators $H_3\mathbf{L^1}$–$H_3\mathbf{L^4}$. The plots showing absorbance at the maximum of the absorption band as a function of time are shown in Fig. S13 and S14.† The measurements were carried out at a molar ratio of Ga : L of 1 : 2 and at 30 °C. The times required for quantitative complexation and the rate constants are shown in Fig. 3 and Table S3.† The complexation kinetics of H_6notP^{Pr} was studied between pH 0 and 2 as the complexation was too fast at pH > 2. At pH 2, H_6notP^{Pr} showed the fastest complexation among the studied chelators. H_3nota showed a significantly slower complexation compared to H_6notP^{Pr} and its complexation rate was studied between pH 1 and 2.5. The experiments were in a good agreement with the previously reported superiority of H_6notP^{Pr} over H_3nota in Ga^{III} complexation rates.[12] The complexation kinetics of $H_3\mathbf{L^1}$ and $H_3\mathbf{L^2}$ was studied at pH 0.5–2.5. Both chelators showed fast complexation at pH < 1.6, although the half-times are higher than those of H_6notP^{Pr}. At pH > 2, the complexation of $H_3\mathbf{L^1}$ and $H_3\mathbf{L^2}$ was significantly slower than that of H_6notP^{Pr} and the half-times of the reaction were more comparable to that of H_3nota. The complexation rates of $H_3\mathbf{L^3}$ and $H_3\mathbf{L^4}$ were studied at pH 1.0–3.0 and 1.6–3.0, respectively. Their complexation rates were comparable. However, these reactions were significantly slower than those of the other phosphinate chelators. This might be ascribed to the presence of a positive charge on the protonated aminomethyl groups of the phosphinate pendant arms. The inhibitory effect of the protonated pendants was so significant that both chelators showed even a slower complexation than H_3nota at almost all pH points.

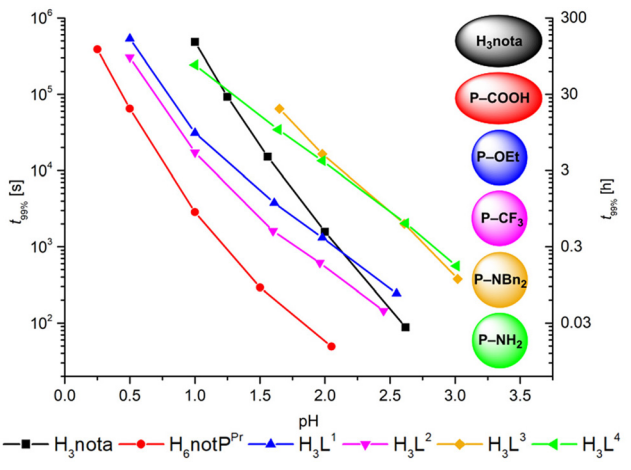

Fig. 3 The times necessary for 99% complexation, $t_{99\%}$, with the studied chelators as a function of pH (c_{chel} = 0.4 mM, c_{Ga} = 0.2 mM, 30 °C, pH 0.25–3.0). The lines serve only as guides to the eye.

The complexation of metal ions by macrocyclic chelators with coordinating pendant arms proceeds in two steps.[31] The first step is the formation of an intermediate *out-of-cage* complex in which the metal ion is bound only to the donor atoms in the pendant arms and the macrocycle amine group(s) are protonated. The second step is the deprotonation of the macrocycle amines with simultaneous transfer of the metal ion into the macrocyclic cavity, forming the final *in-cage* complex. This step is typically the rate-limiting step and is base-catalyzed. Thus, the complexation rate increases with the increasing pH which agrees with the results observed here. The ligand deprotonation in the rate-limiting step indicates that the macrocycle basicity is an important factor. The high basicity of the ring amino groups in H_3nota might explain its slow complexation compared to the H_6notP^{Pr}, $H_3\mathbf{L^1}$ and $H_3\mathbf{L^2}$ complexation. However, the ligand basicity did not correlate with the differences in complexation rates among the phosphinate ligands. Thus, an important role had to be ascribed to the thermodynamic stability of the *out-of-cage* intermediate as the overall reaction rate was also proportional to its concentration. The high stability and, consequently, the high *out-of-cage* complex abundance might be the reason for the fastest H_6notP^{Pr} complexation among the studied ligands as the phosphinato-propionate pendant arms allow for chelating coordination in the *out-of-cage* complex.[6] A structure showing such coordination was previously reported for the *out-of-cage* Gd^{III} complex of the H_4dota analogue bearing four phosphinato-propionate pendant arms.[32] On the other hand, the pendant arm amino groups in $H_3\mathbf{L^3}$ and $H_3\mathbf{L^4}$ were protonated in acidic solutions. The low affinity of the Ga^{III} ion to the nitrogen donor groups and its repulsion with the positively charged protonated amines probably resulted in low stability and, consequently, in low abundance of the *out-of-cage* Ga^{III}–$H_3\mathbf{L^3}$ and Ga^{III}–$H_3\mathbf{L^4}$ complexes. It explains the slow *in-cage* complex formation for these ligands.

In the very low concentrations of all reactants during radiolabelling, the higher abundance (*i.e.* higher thermodynamic stability) of the *out-of-cage* complexes was a very important parameter as it allows a close approach of the diluted metal radioisotope to the ligand cavity. The difference in accessibility of the *out-of-cage* complexes was highlighted in the radiolabelling experiments discussed below.

Radiolabelling with ^{68}Ga

The ^{68}Ga radiolabelling properties of the studied chelators were compared to those of H_3nota and H_6notP^{Pr} both being the current standards for ^{68}Ga radiolabelling. The radiolabelling was performed at various pH values, temperatures, and chelator concentrations according to the established protocols.[6,33,34] The

radiolabelling yields (RCYs) as a function of pH (at 95 °C) are shown in Fig. 4A. Chelators H_3L^1 and H_3L^2 behaved very similar to H_6notP^{Pr} – their RCYs were almost quantitative at pH > 1 and they decreased to ~20% at pH 0.5. Ligands H_3L^3 and H_3L^4 behaved similar to H_3nota and they show lower RCYs than H_3L^1 and H_3L^2. They required pH > 2.0 to achieve good radiolabelling; however, even under the most optimal conditions at pH 3, their RCYs did not exceed ~95% after five minutes. The differences between the chelators were most pronounced at pH 1 where H_3L^1 and H_3L^2 achieved quantitative RCYs whereas the radiolabelling of H_3L^3 and H_3L^4 does not exceed 30%.

The RCYs as a function of the chelator concentration (or more correctly, a function of chelator molar excess over a molar amount of the metal radionuclide) at 95 °C are shown in Fig. 4B. H_3L^1 and H_3L^2 were labelled with high RCYs at concentrations >0.1 μM which was comparable to that of H_6notP^{Pr}. Their RCYs at a concentration of 0.1 μM were over 90% and the RCY decreased rapidly at concentrations lower than 0.01 μM. H_3L^3 and H_3L^4 exhibited significantly lower radiochemical yields at low concentrations. H_3L^4 showed a slightly higher RCY than H_3L^3 but RCYs of both ligands steeply decreased at concentrations lower than 1 μM and the efficiency of both chelators was comparable to that of H_3nota.

The RCYs as a function of temperature at pH 3 are shown in Fig. 4C. The H_3L^1 and H_3L^2 as well as H_3nota and H_6notP^{Pr} exhibited high radiochemical yields even at low temperatures (>80% at 35 °C). In contrast, RCYs of H_3L^3 and H_3L^4 were good only at high temperatures (<70 °C) and significantly decreased with decreasing temperature. The RCY changes with temperature were similar for both chelators, H_3L^3 and H_3L^4.

The role of time in the radiolabelling process was followed at decreased pH (pH = 1) to emphasize differences between the chelators. The experiments were conducted between 2.5 min and 20 min as the times are relevant for practical radiolabelling with ^{68}Ga (Fig. 4D). Ligands H_3L^1, H_3L^2 and H_6notP^{Pr} showed an almost quantitative radiolabelling even after 2.5 minutes. In contrast, H_3L^3 and H_3L^4 were radiolabelled significantly slower and had radiochemical yields of ~80% even after twenty minutes and the benzylated derivative H_3L^3 reacted slightly slower. However, all chelators achieved

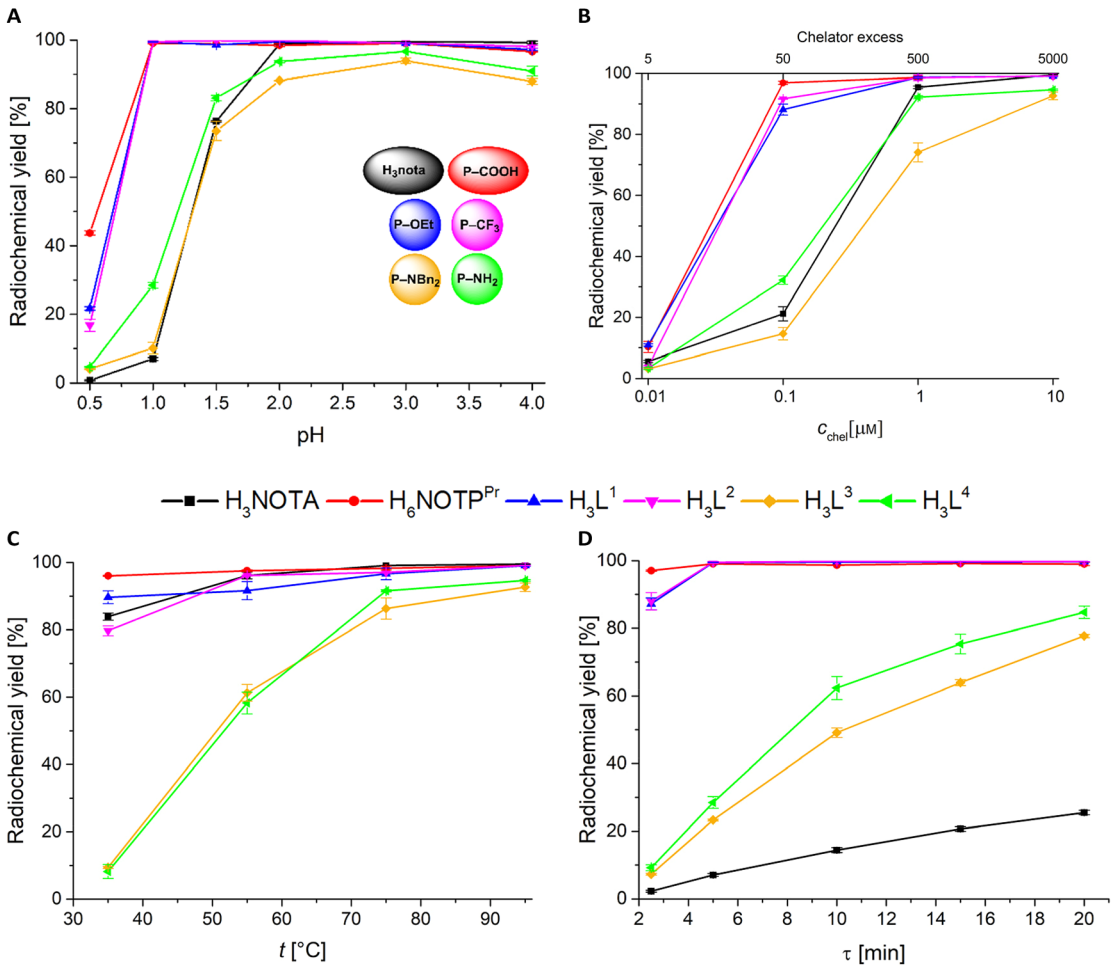

Fig. 4 Radiolabelling of the studied chelators with ^{68}Ga (20–30 MBq ~ 0.2–0.3 pmol ^{68}Ga, 95 °C) as a function of pH (A: c_{chel} = 10 μM ~ n_{chel} = 1 nmol, Ga : L ~ 1: 5000, t = 5 min), chelator concentration (B: 95 °C, pH 3.0, t = 5 min), temperature (C: c_{chel} = 10 μM ~ n_{chel} = 1 nmol, Ga : L ~ 1 : 5000, pH 3, t = 5 min) and time (D: 95 °C, c_{chel} = 10 μM ~ n_{chel} = 1 nmol, Ga : L ~ 1 : 5000, pH 1.0).

higher radiochemical yields than H_3nota showing by far the slowest radiolabelling at such a low pH.

The results of ^{68}Ga radiolabelling showed the same trends as those obtained from the UV-Vis complexation studies. In both experiments, TRAP-ligands dominated over H_3nota at pH < 1.5. However, H_3nota showed a higher relative acceleration of ^{68}Ga labelling with increasing pH than the TRAP-ligands, which might be related to the deprotonation of the carboxylate groups in H_3nota in the studied pH range. Similarly, protonation of *P*-methylamino groups in the pendant arms of $H_3\mathbf{L^3}$ and $H_3\mathbf{L^4}$ resulted in a much less efficient radiolabelling compared to the other TRAP-ligands. The H_3nota, $H_3\mathbf{L^3}$ and $H_3\mathbf{L^4}$ showed also much slower radiolabelling at low ligand concentrations whereas H_6notP^{Pr}, $H_3\mathbf{L^1}$ and $H_3\mathbf{L^2}$ dominated at low pH as well as at low ligand concentrations. These results indicate that protonation of the pendant arms which prevents the formation of the *out-of-cage* intermediates is a key negative factor for the complexation rates and, mainly, for the radiolabelling yields. Thus, chelators able to form relatively stable/abundant *out-of-cage* complexes, H_6notP^{Pr} and H_3nopo, exhibited the best radiolabelling efficiency.[6,10,11]

Conclusion

A new method for the determination of Ga^{III} complexation rates with NOTA-like chelators at μM–mM concentrations ("chemical conditions") was developed and validated. The method is based on UV-Vis quantification of the Cu^{II} complex formed with a non-complexed chelator at individual time points. The method is an easy and cheap tool to follow the kinetics of complexation reactions of metal ions having no UV-Vis absorption under equimolar conditions as well as under a ligand or a metal ion excess. The method was used to study the kinetics of complexation reactions of the Ga^{III} ion with four phosphi(o)nate analogues of H_3nota and the complexation rates were compared with those for Ga^{III}–H_3nota and Ga^{III}–H_6notP^{Pr} systems. Radiolabelling with ^{68}Ga was studied for the same chelators. The data from the chemical and radiochemical experiments followed the same trends and, thus, the "chemical" data could reasonably predict the chelator behavior in radiolabelling. The results further pointed to the importance of the groups attached to the phosphorus atoms in the complexation kinetics/radiolabelling. The H_6notP^{Pr} bearing coordinating carboxylate groups showed the fastest complexation and the highest radiochemical yields. In contrast, complexes of the aminomethylphosphinate derivatives were formed slowly due to electrostatic repulsion between the protonated amino groups and the Ga^{III} cation resulting in a low abundance of *out-of-cage* intermediates. The complexation rates and the radiolabelling efficiencies of the ligands bearing the non-coordinating and non-charged substituents (ethoxy or 2,2,2-trifluoroethyl) were between those of H_6notP^{Pr} and the aminomethylphosphinate derivatives. It indicates that the right choice of substituents on the phosphorus atoms plays a crucial role in the complexation kinetics.

Experimental

Materials and methods

Commercially available chemicals with synthetic purity were used as received. The [(*N*,*N*-dibenzylamino)methyl]-*H*-phosphinic acid (**3**),[24] (2,2,2-trifluoroethyl)-*H*-phosphinic (**2**) and $H_3\mathbf{L^2}$ were synthesized according to the literature.[23] The characterization NMR measurements (^{1}H, ^{13}C{^{1}H}, ^{19}F, ^{31}P, ^{31}P{^{1}H}, ^{71}Ga) were performed on a Bruker Avance III HD (9.4 T, 400 MHz). ^{1}H and ^{13}C{^{1}H} characterization of $H_3\mathbf{L^3}$ was performed on a Bruker Avance III (14.3 T, 600 MHz) and ^{31}P and ^{31}P{^{1}H} characterization was performed on a Varian VNMRS300 (7.0 T, 300 MHz). The ^{1}H and ^{13}C{^{1}H} spectra were referenced to an internal standard *t*BuOH in D_2O (δ_H 1.24 ppm; δ_C 30.3 ppm); ^{19}F spectra were referenced to an external standard containing 0.1 M TFA (δ_F −75.51 ppm); ^{31}P/^{31}P{^{1}H} spectra were referenced to external 85% aq. H_3PO_4 (δ_P 0.0 ppm); ^{71}Ga spectra were referenced to $Ga(NO_3)_3$ (δ_{Ga} 0.0 ppm) in 8 M HNO_3/D_2O or to $[Ga(OH)_4]^-$ (δ_{Ga} 222.4 ppm) in 1 M NaOD/D_2O. The mass spectra were recorded on a Waters ACQUITY QDa spectrometer equipped with an electrospray ionization source and a quadrupole detector. The HR-MS spectra (negative mode, electrospray ionization) were recorded on a Bruker APEX-Q FT-MS.

Synthesis

Hexaethyl 1,4,7-triazacyclononane-1,4,7-tris(methylphosphonate) (1). 1,4,7-Triazacyclononane (2.03 g, 15.5 mmol) and paraformaldehyde (1.74 g, 58.1 mmol) were dissolved in triethyl phosphite (15 ml). The reaction mixture was heated at 40 °C for 3 d. The volatiles were evaporated in a vacuum and the product was purified on a strong cation-exchange resin (Dowex 50, ∼400 ml, H^+-form, elution EtOH → EtOH/conc. aq. ammonia 3 : 1). The impurities were eluted with EtOH, and the product was eluted with EtOH/ammonia solution. The product-containing fraction was evaporated in a vacuum to yield a yellowish oil (8.02 g, 89%).

^{1}H NMR ($CDCl_3$): δ 1.29 (C**H**$_3$–CH$_2$, t, $^3J_{HH}$ 7.1 Hz, 18H), 2.93 (N–C**H**$_2$–C**H**$_2$–N, s, 12H), 2.96 (N–C**H**$_2$–P, d, $^2J_{HP}$ 9.2 Hz, 6H), 4.08 (m, 12H, CH$_3$–C**H**$_2$). ^{31}P{^{1}H} NMR: δ 26.4 (s). MS$^+$: 580.2 $[M + H]^+$ (calc. 579.3).

Triethyl 1,4,7-triazacyclonoane-1,4,7-tris(methylphosphonate) ($H_3\mathbf{L^1}$). The hexaethyl ester **1** (3.98 g, 6.9 mmol) was dissolved in 10% aq. NaOH (50 ml). The reaction mixture was heated at 50 °C for 24 h. The volatiles were evaporated in a vacuum and the product was purified on a strong cation exchange resin (Dowex 50, ∼500 ml, H^+-form, elution with H_2O). The product-containing fraction was evaporated, the resulting oil was re-dissolved in water (100 ml) and lyophilization yielded $H_3\mathbf{L^1}\cdot 1.5H_2O$ in the form of a slightly yellowish hygroscopic powder (1.80 g, 53%).

^{1}H NMR (D_2O, pD 1.0): δ 1.29 (C**H**$_3$–CH$_2$, t, $^3J_{HH}$ 7.1 Hz, 9H), 3.37 (N–C**H**$_2$–P, d, $^2J_{HP}$ 11.0 Hz, 6H), 3.59 (N–C**H**$_2$–C**H**$_2$–N, s, 12H), 4.02 (CH$_3$–C**H**$_2$, m, 6H). ^{13}C{^{1}H} (D_2O, pD 1.0): δ 16.7 (**C**H$_3$–CH$_2$, d, $^3J_{CP}$ 5.7 Hz), 51.7 (N–**C**H$_2$–**C**H$_2$–N, d, $^3J_{CP}$ 6.0 Hz), 52.4 (N–**C**H$_2$–P, d, $^1J_{CP}$ 138.5 Hz), 62.5 (CH$_3$–**C**H$_2$, d, $^2J_{CP}$ 6.1 Hz). ^{31}P (D_2O, pD 1.0) δ 14.4 (bs). ^{31}P{^{1}H} (D_2O, pD 1.0) δ 14.35 (s).

Elemental analysis ($C_{15}H_{35}N_3NaO_9P_3 \cdot 1.5H_2O$, M_r 527.37): C 33.09% (33.25%), H 7.04% (7.07%), N 7.72% (7.45%). MS^+: 496.3 $[M + H]^+$, 991.7 $[2M + H]^+$. MS^-: 494.2 $[M - H]^-$ (calc. 495.2).

1,4,7-Triazacyclononane-1,4,7-tris{methyl-[(*N*,*N*-dibenzylamino)methyl]phosphinic acid} (H_3L^3). 1,4,7-Triazacyclononane (100 mg, 770 μmol) and **3** (790 mg, 2.81 mmol) were dissolved in 6 M aq. HCl (10 ml) and paraformaldehyde (103 mg, 3.43 mmol) was added. The reaction mixture was heated in a closed flask at 40 °C for 18 h. The volatiles were evaporated in a vacuum, the resulting oil was dissolved in 5% aq. ammonia (60 ml) and the mixture was extracted with CH_2Cl_2 (50 ml). The organic phase was dried with Na_2SO_4 and evaporated in a vacuum. The resulting oil was dissolved in a mixture of water (4 ml) and MeOH (4 ml) and purified on a strong cation resin (Dowex 50, ~130 ml, H^+-form, elution with H_2O → 1% aq. pyridine → 20% aq. pyridine). The fraction eluted with 20% pyridine was evaporated in a vacuum and repeatedly co-evaporated with water to remove any traces of pyridine. The oily residue was dissolved in a mixture of acetonitrile (30 ml) and water (100 ml) and the solution was lyophilized. The product was obtained as a hydrate $H_3L^3 \cdot 3H_2O$ (680 mg, 84%).

^1H NMR (D_2O, pD 1.9): δ 2.98 (N–C**H**$_2$–P, d, 6H, $^2J_{HP}$ 7 Hz,), 3.18 (P–C**H**$_2$–NBn$_2$, d, 6H, $^2J_{HP}$ 9 Hz), 3.30 (N–**C**H$_2$–**C**H$_2$–N, s, 12H), 4.41 (C**H**$_2$–Ph, s, 12H), 7.45–7.54 (**H**-arom., m, 30H). $^{13}C\{^1H\}$ NMR (D_2O, pD 1.9): δ 50.8 (P–**C**H$_2$–NBn$_2$, d, $^1J_{CP}$ 87 Hz), 52.9 (N–**C**H$_2$–**C**H$_2$–N, s), 57.0 (N–**C**H$_2$–P, d, $^1J_{CP}$ 101 Hz), 59.9 (**C**H$_2$–Ph, s), 129.3 (**C**-arom., s), 130.2 (**C**-arom., s), 131.1 (**C**-arom., s), 132.2 (**C**-arom., s). ^{31}P NMR (D_2O, pD 1.9): δ 20.7 (m, $^2J_{HP}$ 7 Hz, $^2J_{HP}$ 9 Hz). $^{31}P\{^1H\}$ (D_2O, pD 1.9): δ 20.7 (s). Elemental analysis ($C_{54}H_{69}N_6O_6P_3 \cdot 3H_2O$, M_r 1045.1): C 62.1 (61.8), H 7.2 (7.0), N 8.0 (8.0), MS^+: 991.1 $[M + H]^+$, 1013.0 $[M + Na]^+$, 1035.1 $[M + 2Na - H]^+$, MS^-: 989.63 $[M - H]^-$ (calc. 990.4).

1,4,7-Triazacyclonoane-1,4,7-tris[methyl-(aminomethyl) phosphinic acid] (H_3L^4). $H_3L^3 \cdot 3H_2O$ (691 mg; 661 μmol) was dissolved in a mixture of water (70 ml) and concentrated aq. ammonia (0.65 ml), and $(NH_4)H_2PO_2$ (1.74 g; 21.0 mmol) and catalyst (10% Pd/C, 207 mg; 195 μmol) were added. The mixture was stirred at 60 °C for 22 h. After cooling to room temperature, the solids were filtered off on a fine frit and washed with water (5 ml). The filtrate was evaporated, and the resulting oil was dissolved in water and re-evaporated. The crude product was purified on a strong cation exchange resin (Dowex 50, ~100 ml, H_2O → 1% aq. pyridine → 20% aq. pyridine). The fractions eluted with 20% pyridine containing a pure product were combined, volatiles were evaporated in a vacuum and the residue was repeatedly co-evaporated with water to remove any traces of pyridine. The resulting oil was dissolved in water (40 ml) and lyophilization yielded $H_3L^4 \cdot 2.5H_2O$ in the form of a white powder (182 mg; 56%).

^1H NMR (D_2O, pD 8): δ 3.05 (P–C**H**$_2$–NH$_2$, d, 6H, $^2J_{HP}$ 9.0 Hz), 3.14 (N–C**H**$_2$–C**H**$_2$–N, s, 12H), 3.22 (N–C**H**$_2$–P, d, 6H, $^2J_{HP}$ 6.4 Hz). $^{13}C\{^1H\}$ (D_2O, pD 8): δ 38.9 (P–**C**H$_2$–NH$_2$, d, $^1J_{CP}$ 91 Hz), 51.8 (N–**C**H$_2$–**C**H$_2$–N, d, $^3J_{CP}$ 4.3 Hz), 54.7 (N–**C**H$_2$–P, d, $^1J_{CP}$ 99.3 Hz). ^{31}P (D_2O, pD 8): δ 27.6 (m, $^2J_{HP}$ 9.0 Hz, $^2J_{HP}$ 6.4 Hz). $^{31}P\{^1H\}$ (D_2O, pD 8): δ 27.6 (s). Elemental analysis ($C_{12}H_{33}N_6O_6P_3 \cdot 2.5H_2O$, M_R 495.4): C 29.1 (29.2), H 7.7 (7.3), N 17.0 (16.8). MS^+: 451.36 $[M + H]^+$, 473.28 $[M + Na]^+$, 489.24 $[M + K]^+$, 901.50 $[M + H]^+$. MS^-: 249.00 $[M - 2H]^{2-}$, 449.27 $[M - H]^-$ (calc. 450.2).

[GaL^1]: $Ga(NO_3)_3 \cdot xH_2O$ (40 mg, ~100 μmol) was dissolved in water (5 ml) and concentrated aq. ammonia (1 ml) was added. The precipitate was separated by centrifugation, repeatedly washed with water and centrifuged. The resulting material was suspended in a solution of $H_3L^1 \cdot 1.5H_2O$ (20.1 mg, 38 μmol) in water (2 ml). The mixture was stirred at room temperature overnight. The excess of the solid $Ga(OH)_3$ was filtered off with a microfilter and the filtrate was evaporated in a vacuum yielding [**GaL^1**] as a hygroscopic oil (32 mg). The complex was characterized by ^1H, $^{13}C\{^1H\}$, ^{31}P, $^{31}P\{^1H\}$, ^{71}Ga NMR and MS (Fig. S7 and S8†).

^1H NMR (D_2O, pD 7.6): δ 1.31 (C**H**$_3$–CH$_2$, m, 9H), 3.0–3.7 (N–C**H**$_2$–P + N–C**H**$_2$–C**H**$_2$–N, m, 18 H), 4.15 (CH$_3$–C**H**$_2$, m, 6H). $^{13}C\{^1H\}$ (D_2O, pD 7.6): δ 16.4 (**C**H$_3$–CH$_2$, m), 53.1 (m), 55.3 (m), 56.6 (m), 63.7 (m), 64.6 (m). ^{31}P (D_2O, pD 7.6): δ 20.7 (bs), 21.2 (bs). $^{31}P\{^1H\}$ (D_2O, pD 7.6): δ 20.7 (bs), 21.2 (bs). ^{71}Ga (D_2O, pD 7.6): 120.3 (s, $\nu_{1/2}$ = 218 Hz). HR-MS^-: 560.06087 $[M - H]^-$ (calc. 560.06127).

[GaL^2]: $Ga(NO_3)_3 \cdot xH_2O$ (40 mg, ~100 μmol) was dissolved in water (5 ml) and concentrated aq. ammonia (1 ml) was added. The precipitate was separated by centrifugation and repeatedly washed with water and centrifuged. The resulting material was suspended in a solution of H_3L^2 (20.3 mg, 33 μmol) in water (2 ml) and the mixture was stirred at room temperature overnight. The solid $Ga(OH)_3$ was filtered off with a microfilter, and water was evaporated in a vacuum yielding 25.6 mg of pure [**GaL^2**] as a hygroscopic oil. The complex was characterized by ^1H, $^{13}C\{^1H\}$, ^{19}F, ^{31}P, $^{31}P\{^1H\}$ and ^{71}Ga NMR and MS (Fig. S9 and S10†).

^1H NMR (D_2O, pD 5.4): δ 2.98 (P–C**H**$_2$–CF$_3$, dq, $^2J_{HP}$ 16.0, $^3J_{HF}$ 11.0 Hz, 6H), 3.08–3.60 (N–C**H**$_2$–P, N–C**H**$_2$–C**H**$_2$–N, m, 18H). $^{13}C\{^1H\}$ (D_2O, pD 5.4): δ 37.5 (P–**C**H$_2$–CF$_3$, dq, $^1J_{CP}$ 96.5 Hz, $^2J_{CF}$ 29.5 Hz), 54.2 (N–**C**H$_2$–CH$_2$–N, s), 57.6 (N–CH$_2$–**C**H$_2$–N, d, $^3J_{CP}$ 13 Hz) 60.8 (N–**C**H$_2$–P, d, $^1J_{CP}$ 92.0 Hz), 126.8 (P–CH$_2$–**C**F$_3$, qd, $^1J_{CF}$ 276.0 Hz, $^2J_{CP}$ 3 Hz). ^{31}P (D_2O, pD 5.4): δ 30.67 (bs). $^{31}P\{^1H\}$ (D_2O, pD 5.4): δ 30.67 (q, $^3J_{FP}$ 11 Hz). ^{19}F (D_2O, pD 5.4): −57.29 (m, $^3J_{FP}$ 11.1 Hz, $^3J_{FH}$ 11.0 Hz). ^{71}Ga (122 MHz): 136.2 (s, $\nu_{1/2}$ = 236 Hz). HR-MS^-: 673.99115 $[M - H]^-$ (calc. 673.99173).

[GaL^3]: $H_3L^3 \cdot 3H_2O$ (25.0 mg 24 μmol) was dissolved in water (1 ml) and $Ga(NO_3)_3 \cdot xH_2O$ (8.2 mg, ~27 μmol) was added. The formed precipitate was filtered, washed with water and dried on air. A low complex solubility disabled common spectral characterization. MS^+: 1057.8 $[M + H]^+$ (calc. 1056.4).

[GaL^4]: $H_3L^4 \cdot 2.5H_2O$ (12.5 mg, 25 μmol) was dissolved in water (1 ml) and $Ga(NO_3)_3 \cdot xH_2O$ (11.2 mg, ~37 μmol) was added. The pH was adjusted to pH 3.5 with aq. LiOH. The mixture was stirred at 50 °C overnight and pH was adjusted to 5.6 with aq. LiOH. Precipitated $Ga(OH)_3$ was filtered off with a microfilter and water was evaporated in a vacuum yielding 16.5 mg of pure [**GaL^4**] as a hygroscopic oil. The complex was

characterized by ^{1}H, ^{13}C{^{1}H},^{31}P, ^{31}P{^{1}H} and ^{71}Ga NMR and MS (Fig. S11 and S12†).

^{1}H NMR (D_2O, pD 7.6): δ 2.9–3.6 (m). ^{13}C{^{1}H} (D_2O, pD 7.6): δ 39.7 (P–**C**H$_2$–NH$_2$, d, $^{1}J_{CP}$ 104.6 Hz), 53.1 (N–**C**H$_2$–CH$_2$–N, s), 56.5 (N–CH$_2$–**C**H$_2$–N, d, $^{3}J_{CP}$ 13 Hz), 56.9 (N–**C**H$_2$–P, d, $^{1}J_{CP}$ 82.4 Hz). ^{31}P (D_2O, pD 7.6): δ 38.68 (m). ^{31}P{^{1}H} (D_2O, pD 7.6): δ 38.68 (s). ^{71}Ga (D_2O, pD 7.6): 137.6 (s, $\nu_{1/2}$ = 320 Hz). HR-MS^{-}: 515.06157 $[M - H]^{-}$ (teor. 515.06227).

Potentiometry

Potentiometry was carried out according to the previously published procedures; for the preparation of the stock solutions, equipment, electrode system calibration, titration procedures and data treatment, see ref. 3 and 35. Throughout the paper, pH means –log[H^{+}]. The concentration protonation constants were determined in 0.1 M (NMe_4)Cl at 25.0 °C with pK_w = 13.81 by in-cell titrations from data obtained in the pH range 1.6–12 with ~40 points per titration and four parallel titrations (c_L = 0.004 M). The constants were calculated with the OPIUM program.[36]

Formation kinetics

The formation kinetics of Ga^{III} complexes was studied in aqueous solution at 30 °C, c_{chel} = 0.4 mM and c_{Ga} = 0.2 mM. The experiments at pH 0.25–1.50 were performed in aq. $HClO_4$ (pH was calculated using the $HClO_4$ concentration), at pH 2.00 in aq. 0.1 M betaine/HCl buffer, and at pH values of 2.50 and 3.00 in aq. 0.1 M HEPES/HCl buffer. At each time point, the solution aliquot (400 µl) was transferred into a vial with $CuSO_4$ solution (400 µl, 1.25 mM) in aq. 1 M HEPES/HCl buffer (pH 3). The mixture was incubated for 5 min at room temperature and UV-Vis spectra were recorded (190–400 nm) on a Specord 50 Plus system (Analytic Jena). The rate constants and the reaction times were obtained from the absorbance at 265 nm (280 nm in the case of $H_3\mathbf{L}^{3}$) according to eqn (1).

$$A = A_\infty + (A_0 - A_\infty) \times e^{-kt} \quad (1)$$

^{1}H NMR experiments were performed on the Ga^{III}–$H_3\mathbf{L}^{2}$ system at 30 °C (c_{chel} = 0.4 mM, c_{Ga} = 0.2 mM and pH 1.00 given by aq. 0.1 M $HClO_4$) on a Bruker Avance III (14.3 T, 600 MHz). The water signal was suppressed by excitation sculpting. The rate constant and the reaction times were obtained from the integral intensity of the P–C**H**$_2$–CF_3 signal of the free chelator according to eqn (2).

$$I = I_\infty + (I_0 - I_\infty) \times e^{-kt} \quad (2)$$

Radiolabelling

Radiolabelling was studied in triplicate by a manual synthesis under different conditions (pH, chelator concentration, temperature and time). A ^{68}Ge/^{68}Ga-generator (Eckert & Ziegler) was eluted with 1.0 M aq. HCl. A fraction of 1.25 ml with the highest activity of 300–450 MBq was added to 2 M aq. HEPES/HCl (60 µl). Then, pH was adjusted with 1 M aq. HCl and 1 M aq. NaOH (the final pH 0.5–4). A solution aliquot (90 µl, 20–30 MBq) was transferred to a preheated Eppendorf tube containing an aqueous solution of the chelator (10 µl). The resulting chelator concentrations were 10^{-5}–10^{-8} M. Incorporation of ^{68}Ga was determined by radio-TLC on TLC-paper impregnated with silica-gel (Agilent Technologies, mobile phase 1 : 1 1 M aq. (NH_4)OAc : MeOH (v/v)). The radioactivity incorporation was evaluated using a BIOSCAN TLC scanner with Bio-chrom Lite software.

Data availability

The data supporting this article have been included as part of the ESI.†

Conflicts of interest

There are no conflicts to declare.

Acknowledgements

The support from the Technology Agency of the Czech Republic (TAČR TH78020003) and the Grant Agency of the Charles University (GAUK 1501/2024) is acknowledged. The stay of V. L. at Technical University Munich was supported by the Foundation of the Faculty of Science of Charles University (Prague). We thank Dr J. Havlíčková for performing the potentiometric titrations.

References

1 G. I. Gleason, *Int. J. Appl. Radiat. Isot*, 1960, **8**, 90.
2 B. J. B. Nelson, J. D. Andersson, F. Wuest and S. Spreckelmeyer, *EJNMMI Radiopharm. Chem.*, 2022, **7**, 27.
3 V. Kubíček, J. Havlíčková, J. Kotek, G. Tircsó, P. Hermann, E. Tóth and I. Lukeš, *Inorg. Chem.*, 2010, **49**, 10960.
4 P. R. W. J. Davey and B. M. Paterson, *Molecules*, 2023, **28**, 203.
5 M. Fellner, P. Riss, N. Loktinova, K. Zhernosekov, O. Thews, C. F. G. C. Geraldes, Z. Kovacs, I. Lukeš and F. Rösch, *Radiochim. Acta*, 2011, **99**, 43.
6 J. Notni, P. Hermann, J. Havlíčková, J. Kotek, V. Kubíček, J. Plutnar, N. Loktionova, P. J. Riss, F. Rösch and I. Lukeš, *Chem. – Eur. J.*, 2010, **16**, 7174.
7 M. I. M. Prata, J. P. André, Z. Kovács, A. I. Takács, G. Tircsó, I. Tóth and C. F. G. C. Geraldes, *J. Inorg. Biochem.*, 2017, **177**, 8.
8 G. Máté, J. Šimeček, M. Pniok, I. Kertész, J. Notni, H.-J. Wester, L. Galuska and P. Hermann, *Molecules*, 2015, **20**, 13112.
9 J. Notni, J. Šimeček and H.-J. Wester, *ChemMedChem*, 2014, **9**, 1107.
10 J. Šimeček, P. Hermann, H.-J. Wester and J. Notni, *ChemMedChem*, 2013, **8**, 95.
11 J. Šimeček, O. Zemek, P. Hermann, J. Notni and H.-J. Wester, *Mol. Pharmaceutics*, 2014, **11**, 3893.

12 J. Šimeček, M. Schulz, J. Notni, J. Plutnar, V. Kubíček, J. Havlíčková and P. Hermann, *Inorg. Chem.*, 2012, **51**, 577.
13 J. Holub, M. Meckel, V. Kubíček, F. Rösch and P. Hermann, *Contrast Media Mol. Imaging*, 2015, **10**, 122.
14 J.-F. Morfin and É. Tóth, *Inorg. Chem.*, 2011, **50**, 10371.
15 A. Vágner, A. Forgács, E. Brücher, I. Tóth, A. Maiocchi, A. Wurzer, H.-J. Wester, J. Notni and Z. Baranyai, *Front. Chem.*, 2018, **6**, 170.
16 K. Kumar, C. A. Chang and M. F. Tweedle, *Inorg. Chem.*, 1993, **32**, 587.
17 K. Kumar and M. F. Tweedle, *Inorg. Chem.*, 1993, **32**, 4193.
18 H.-Z. Cai and T. A. Kaden, *Helv. Chim. Acta*, 1994, **77**, 383.
19 M. Försterová, I. Svobodová, P. Lubal, P. Táborský, J. Kotek, P. Hermann and I. Lukeš, *Dalton Trans.*, 2007, 535.
20 V. Kubíček, Z. Böhmová, R. Ševčíková, J. Vaněk, P. Lubal, Z. Poláková, R. Michalicová, J. Kotek and P. Hermann, *Inorg. Chem.*, 2018, **57**, 3061.
21 J. Kubinec, V. Širůčková, J. Havlíčková, J. Kotek, V. Kubíček, P. Lubal and P. Hermann, *Eur. J. Inorg. Chem.*, 2022, e202200173.
22 I. Lázár and A. D. Sherry, *Synthesis*, 1995, 453.
23 F. Koucký, T. Dobrovolná, J. Kotek, I. Císařová, J. Havlíčková, A. Liška, V. Kubíček and P. Hermann, *Dalton Trans.*, 2024, **53**, 9267.
24 J. Kotek, P. Lebdušková, P. Hermann, L. Vander Elst, R. N. Muller, C. F. G. C. Geraldes, T. Maschmeyer, I. Lukeš and J. A. Peters, *Chem. – Eur. J.*, 2003, **9**, 5899.
25 D. A. Moore, P. E. Fanwick and M. J. Welch, *Inorg. Chem.*, 1990, **29**, 612.
26 C. Broan, J. P. Cox, A. S. Craig, R. Kataky, D. Parker, A. Harrison, A. M. Randall and G. Ferguson, *J. Chem. Soc., Perkin Trans. 2*, 1991, 87.
27 Z. Kotková, G. A. Pereira, K. Djanashvili, J. Kotek, J. Rudovský, P. Hermann, L. Vander Elst, R. N. Muller, C. F. G. C. Geraldes, I. Lukeš and J. A. Peters, *Eur. J. Inorg. Chem.*, 2009, 119.
28 G. A. Pereira, L. Ball, A. D. Sherry, J. A. Peters and C. F. G. C. Geraldes, *Helv. Chim. Acta*, 2009, **92**, 2532.
29 P. Hermann, J. Kotek, V. Kubíček and I. Lukeš, *Dalton Trans.*, 2008, 3027.
30 I. Lukeš, J. Kotek, P. Vojtíšek and P. Hermann, *Coord. Chem. Rev.*, 2001, **216–217**, 287.
31 E. Brücher, G. Tircsó, Z. Baranyai, Z. Kovács and A. D. Sherry, in *The Chemistry of Contrast Agents in Medical Magnetic Resonance Imaging*, ed. A. Merbach, L. Helm and É. Tóth, Wiley, Chichester, U.K., 2nd edn, 2013, pp. 157–208.
32 J. Šimeček, P. Hermann, J. Havlíčková, E. Herdtweck, T. Kapp, N. Engelbogen, H. Kessler, H.-J. Wester and J. Notni, *Chem. – Eur. J.*, 2013, **19**, 7748.
33 J. Notni, J. Šimeček, P. Hermann and H.-J. Wester, *Chem. – Eur. J.*, 2011, **17**, 14718.
34 M. Asti, G. De Pietri, A. Fraternali, E. Grassi, R. Sghedoni, F. Fioroni, F. Roesch, A. Versari and D. Salvo, *Nucl. Med. Biol.*, 2008, **35**, 721.
35 M. Försterová, I. Svobodová, P. Lubal, P. Táborský, J. Kotek, P. Hermann and I. Lukeš, *Dalton Trans.*, 2007, 535.
36 (*a*) M. Kývala and I. Lukeš, in *International Conference Chemometrics '95*, Pardubice, Czech Republic, 1995, p. 63 (*b*) M. Kývala, P. Lubal and I. Lukeš, in *IX. Spanish-Italian and Mediterranean Congress on Thermodynamics of Metal Complexes (SIMEC 98)*, Girona, Spain, 1998. The full version of the OPIUM program is available (free of charge) on **https://www.natur.cuni.cz/_kyvala/opium.html**.